GEOPHYSICS, VOL. 84, NO. 4 (JULY-AUGUST 2019); P. B259–B268, 8 FIGS., 2 TABLES.
10.1190/GEO2018-0755.1

DOI:10.1190/geo2018-0755.1

Case History

Deep onshore reflection seismic imaging of the chalk group strata using a 45 kg accelerated weight-drop and combined recording systems with dense receiver spacing

Janina Kammann[1], Alireza Malehmir[2], Bojan Brodic[2], Mattia Tagliavento[3], Lars Stemmerik[3], Egon Nørmark[4], Holger Lykke-Andersen[4], and Lars Nielsen[1]

ABSTRACT

The Chalk Group forms important hydrocarbon reservoirs offshore and water aquifers onshore Denmark. Within a day of fieldwork, a 450 m long reflection seismic profile was acquired onshore in an area in southeast Denmark, where the Chalk Group extends almost to the surface and is approximately 900 m thick. The main objective of the study was to image the complete Chalk Group in high resolution and to study the origin of reflectivity within the different chalk units. A 45 kg accelerated weight-drop source, in combination with dense receiver spacing using microelectromechanical sensors mounted on a streamer and 48 planted geophones, was used for data acquisition. The profile runs subparallel to the cliffs of Stevns, and the recorded signal reaches the base of the Chalk Group at approximately 600 ms. The fully cored 443 m-deep Stevns-1 borehole, which is located at the recorded seismic line, provides excellent control on lithologic and facies changes. Comparison with the borehole data demonstrates that our seismic data set provides a high-resolution image of the internal layering of the Chalk Group. We find that the internal reflection coefficients of the Chalk Group are, in general, small based on wireline-log data. However, the reflected amplitudes are just big enough to be recorded with the receiver setup used, even from the pure chalk beds of the Chalk Group. The reflectivity seen on the high-resolution seismic profile is influenced by occurrences of clay-enriched chalk layers. Flint bands consisting of numerous flint nodules are a characteristic of the uppermost part of the Chalk Group at Stevns. The flint nodules appear to produce significant scattering of the seismic signals, and flint-rich layers appear with diffuse internal reflectivity characteristics. Outcrop-scale mound structures in Danian and Upper Cretaceous outcrops are for the first time seismically resolved.

INTRODUCTION

Forming an important reservoir for hydrocarbons in the North Sea and groundwater onshore Denmark, the Danish Chalk Group has been within the scope of extensive geologic and geophysical studies for decades (e.g., Surlyk, 1997; Fabricius, 2003; Hjuler and Fabricius, 2009; Almholt et al., 2013; Smit et al., 2018; van Buchem et al., 2018). Due to strong internal contrasts in rock-physical parameters, high porosities, and high attenuation (Payne et al., 2007), imaging the Chalk Group with reflection seismology is chal-

Manuscript received by the Editor 2 November 2018; revised manuscript received 14 February 2019; published ahead of production 27 March 2019; published online 27 May 2019.
[1]University of Copenhagen, Department of Geoscience and Natural Resource Management, Øster Voldgade 10, Copenhagen K DK-1350, Denmark. E-mail: jkm@ign.ku.dk (corresponding author); ln@ign.ku.dk.
[2]Uppsala University, Department of Earth Sciences, Villavägen 16, Uppsala SE-75236, Sweden. E-mail: alireza.malehmir@geo.uu.se; bojan.brodic@geo.uu.se.
[3]University of Copenhagen, Natural History Museum of Denmark, Øster Voldgade 5-7, Copenhagen 1350, Denmark. E-mail: mtagliavento@snm.ku.dk; lars.stemmerik@snm.ku.dk.
[4]University of Aarhus, Institute for Geoscience, Hoegh-Guldbergs Gade 2, Aarhus C DK 8000, Denmark. E-mail: en@geo.au.dk; hla@geo.au.dk.

DOI:10.1190/geo2018-0755.1

lenging in terms of acquisition techniques, processing, and geologic ties. Therefore, several studies have been carried out to investigate, e.g., pitfalls in seismic velocity analysis, estimate porosity variations, and effects of porosity and hydrocarbons on seismic velocities (e.g., Anderson, 1999; Abramovitz et al., 2010; Montazeri et al., 2018). Using a small seismic impact source and a dense receiver spacing with a combination of geophones and microelectromechanical sensors (MEMS) landstreamer, we present a data set providing new insights on controlling factors of reflectivity of the Chalk Group rocks and resolve new small-scale structural features.

It is well-known that simple instrumental setups, such as using sledgehammers, weight-drops or small explosives, and an array of receivers (planted or landstreamer mounted), are capable of imaging the shallow subsurface in high quality (e.g., Miller et al., 1986; Baker et al., 2000) and in hard rocks sometimes to large depths (e.g., Malehmir et al., 2015). For example, imaging of fracture systems using 10–30 g explosive charges have been reported in the literature (Bergman et al., 2002; Kaiser et al., 2011). The newly acquired data reported in this study are from the Danish island of Sjælland and prove that the methodology can also be successfully applied in sedimentary rocks, such as the fine-grained limestone of the Danish Chalk Group. Furthermore, the relatively broad bandwidth of the impact source together with its successful recording enables a unique opportunity for resolving the internal structures of the Chalk Group.

The usage of landstreamers for reflection seismics have proven to be advantageous in several scientific studies and commercial applications due to their easy handling, dense receiver spacing, and fast data acquisition without the time-consuming need for the planting of geophones (e.g., van der Veen and Green, 1998; Inazaki, 2004; Vangkilde-Pedersen et al., 2006). Most landstreamers are geophone based with natural frequencies of 10–28 Hz; hence, they are band limited between natural (approximately 10–28 Hz or higher) and spurious (<350 Hz) frequency, imposing a shortcoming for broadband data acquisition when impact sources are used. Compared with geophones designed to work above their resonant frequency, MEMS-based sensors have the great advantage of having a theoretically flat-amplitude response for frequencies in the range of 0–800 Hz because they best perform below their resonance frequency (e.g., 1000 Hz) (Maxwell et al., 2001; Brodic et al., 2015; Malehmir et al., 2017). Therefore, MEMS provide a good alternative for broadband data recording in land seismic acquisition.

Thus, the main objectives of this study are to (1) provide a full-depth image of the Chalk Group using a 45 kg accelerated weight-drop and a dense receiver spread by combining a MEMS-based landstreamer with planted geophones, (2) explain the origin of the reflectivity within the Chalk Group, and (3) discuss reasons for results in terms of Chalk Group rock composition, study environment, and such deep imaging within the perceived highly attenuative medium.

STUDY AREA AND EARLIER SURVEYS

The study area of the Stevns peninsula is located approximately 70 km south of Copenhagen at the southeastern margin of the Danish Basin (Figure 1). The basin was formed during the Permian and includes an up to 2000 m thick succession of Upper Cretaceous and Danian chalk (Erlstrom et al., 1997; Vejbæk et al., 2007). The Chalk Group becomes thinner over the Ringkøbing-Fyn High and is approximately 900 m thick in the study area (Lykke-Andersen and Surlyk, 2004; Nielsen et al., 2011). Eastward, the depositional area is separated from the more stable Baltic Shield by the north-northwest–south-southeast-oriented Sorgenfrei-Tornquist Zone (Thybo, 2001). Deposition of the Chalk Group sediments took place on a wide, relatively deep shelf that covered huge areas of northwest Europe and extended eastward as far as the Krim Peninsula. The Upper Cretaceous succession is dominated by pure nannofossil limestone (chalk) with some marly intervals and increasing content of flint upwards (e.g., Surlyk et al., 2013; Boussaha et al., 2016). The youngest, Danian succession is dominated by bryozoan build-ups along the coastal cliffs of the Stevns peninsula (e.g., Bjerager and Surlyk, 2007). Outcropping Danian and Upper Maastrichtian rocks at the cliffs of Stevns were shown to be to some degree analogues to North Sea reservoirs (Ekofisk and Tor Formations) in terms of stratigraphy and their petrophysical variability (Frykman, 2001). At Stevns, the Danian-Campanian part of the Chalk Group has been cored in two, 350–450 m deep boreholes, and detailed facies analysis as well as petrophysical and log data are thus available for the upper half of the succession (see Surlyk et al., 2013). The deepest borehole, Stevns-1 is located less than 19 m from the survey and are therefore well-suited to be tied to the seismic data.

Several studies have been carried out on the Stevns peninsula on Upper Maastrichtian chalk and Danian bryozoan mound structures expressed in the 40 m high cliffs along the coast and adjacent quarries and in neighboring areas (Thomsen, 1976; Surlyk, 1997; Nielsen et al., 2004; Anderskouv et al., 2007; Bjerager and Surlyk, 2007). Mounds of 30–60 m width and 5–10 m height observed within the study area have previously been reported by Nielsen et al. (2004). Although mound structures on the 100 m scale have been mapped in the Chalk Group by marine seismic surveys, outcrop-scale mounds were found not to be resolvable by high-resolution marine seismic data with vertical resolution of 10–15 m (Nielsen et al., 2004).

Nielsen et al. (2011) present a data set of refraction seismics and one reflection seismic profile acquired for studying the compaction and burial history of the Chalk Group by means of velocity variations. East of the study area, Lykke-Andersen and Surlyk (2004) present a marine seismic profile, which is subparallel to our seismic profile line. This profile was acquired in 1999–2000 with a sleeve gun cluster of three synchronized airguns with a total volume of 45 in^3 pressured at 100 bar. A 24 channel streamer with 6.25 m hydrophone group spacing recorded the reflection seismic signal. They found good a signal-to-noise ratio down to the base of the Chalk (BC) Group, but fuzzy near-surface reflections due to multiples from the water column. Moreau et al. (2016) reprocess the seismic profiles to image polygonal faults within the Chalk Group. The fault systems were interpreted to be of early diagenetic origin and occur in zones. The Stevns-2 core suggests that the fault systems identified in the seismic data are genetically linked to hairline fractures.

SEISMIC SURVEY

Data acquisition

A 465 m long reflection seismic profile was acquired in one day of field work in 2016, subparallel to the cliffs of Stevns, 400 m north of an active chalk quarry (Figure 1). Table 1 summarizes the main acquisition parameters of the survey. Most of the profile runs along an asphalt road, whereas the northernmost 150 m part is located on a well-compacted gravel road. Using mainly a 45 kg accelerated weight-drop source (ESS 100, providing approximately

360 J energy, impact velocity likely approximately 4 m/s, according to the manufacturer), approximately 360 shot records were generated near the receiver positions (Figure 2). Only at a few places was a 5 kg sledgehammer used as the seismic source. At each shot position, on average 4 m apart, three shot records were generated and vertically stacked to provide a better signal-to-noise ratio. A combination of a landstreamer with 100 3C MEMS sensors (236 m long with 2 and 4 m receiver spacing) and 48 wireless recorders connected to 10 Hz vertical geophones were used for the data acquisition. Prior to deploying the landstreamer, the 10 Hz geophones with wireless recorders were deployed with 10 m spacing to cover the entire spread. This provides a better fold at locations where the streamer moved to a new position with an 18 m overlap, along with longer offsets for traveltime tomography purposes (Figure 2; Table 1). Data merging between landstreamer and wireless recorders were facilitated based on GPS-time stamping of shots from the landstreamer data. The wireless recorded geophone and landstreamer data were merged prior to vertical stacking and used further for data processing. In the northernmost part of the profile, only wireless geophone recorders were used due to logistical/topographical issues.

Data processing

Before data processing, the vertical component of the 3C landstreamer was isolated because P-wave reflection imaging was intended. Comparison of the frequency spectra of the MEMS-based sensors (accelerometer; receiver location 100–200) and the geophones (velocity meter; receiver location 1–48), shows a clearly higher content of high frequencies in the MEMS data with respect to the 10 Hz geophones (Figure 3a, frequency spectrum of wireless versus landstreamer data). The noise level of the data is comparable for receivers with the same offsets because the geophones were planted along the landstreamer spread (Table 1). Considering the broader bandwidth of the MEMS, we used a spectral balancing filter in the range of 50–70–250–300 Hz with a 30 Hz window and a 13 ms gapped deconvolution to equalize the two receiver types. We later illustrate phase and amplitude consistency when we compare stacked sections with and without the wireless (geophone) data.

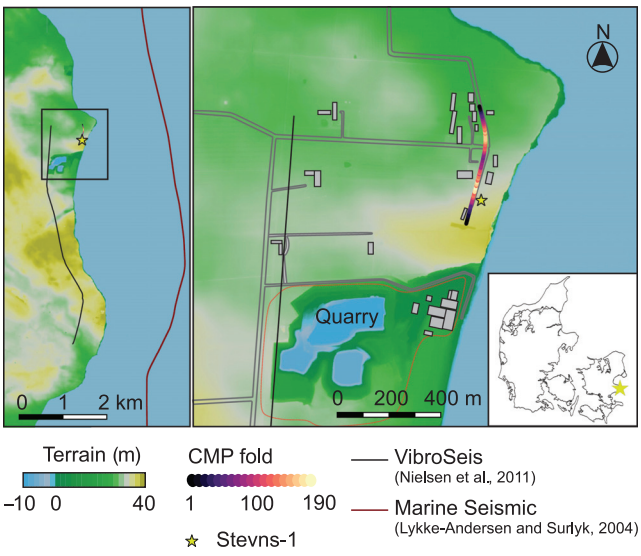

Figure 1. Map of the study area with profile location marked with the corresponding CMP fold. Directly south of the newly acquired profile is an active chalk quarry, outlined in red.

Table 1. Acquisition parameters.

Survey parameters	
Acquisition type	Swath with two streamer positions + fixed planted geophones (wireless)
Acquisition system	Sercel Lite 428 (GPS time stamping)
Source	45 kg accelerated weight drop
Shot interval	4 m
Source pattern	Three records/shotpoint
Number of shots	Approximately 360 (120 after vertical stacking)
Number of receivers	100-3C MEMS in the streamer 48-1C 10 Hz geophones (planted, wireless recorders)
Landstreamer setup (MEMS)	20 units with 4 m spacing 80 units with 2 m spacing 236 m total length
Wireless recorders (geophone)	Fixed 10 m spacing along the whole profile
Maximum offset	Approximately 500 m
Number of streamer positions	2 (18 m overlap)
Profile length	465 m
Recording parameters	
Record length	2 s
Sampling rate	1 ms
Number of traces	Approximately 17,760 (after vertical stacking)

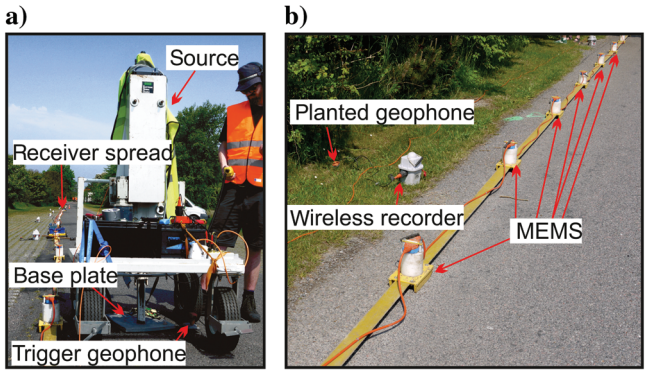

Figure 2. Field photos from the seismic survey, (a) 45 kg accelerated weight-drop source with metal base plate, and (b) MEMS-sensors mounted on the landstreamer and 1C-10 Hz geophones connected to the wireless recorders used to acquire the seismic data. Wireless recorders operated in an autonomous mode. GPS-times of the active sources recorded on the MEMS-sensors were used to harvest the corresponding data from the wireless units.

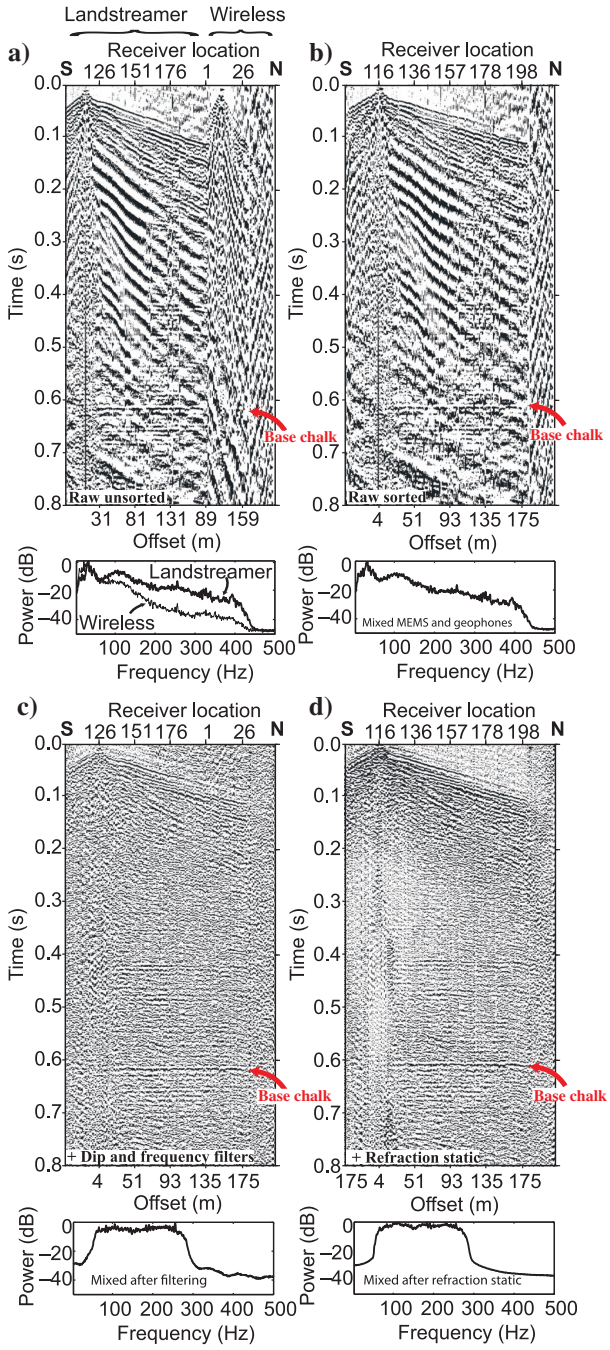

Figure 3. An example shot record illustrating effect of the applied processing steps improving sharpness and strength of reflectivity. (a) Unsorted raw data (after vertical stacking of the repeated records) with the vertical component of the MEMS at receiver locations 101–200 (receiver spacing 2–4 m) and wireless geophone units at receiver locations 1–48 (receiver spacing 10 m). (b) Raw data sorted by offset; note the consistency in the first-break phase between the geophone and the MEMS data. Geophone data clearly show lower frequency content as visually evident in the record, but also in the amplitude spectrum (a). (c) The same shot record as (a), but after a few processing steps, including band pass, spectral equalization, deconvolution, and f-k filters, (d) refraction static corrections. Note the continuity of the reflections at 600 ms and those highly recovered at earlier arrival times. Up to 300 Hz frequencies were kept and judged to be useful for reflection imaging and preprocessed data, as shown in Table 2.

A prominent reflection event at approximately 600 ms can easily be identified in the data, although strong surface waves (from near-surface heterogeneities, waves on the shoreline, and a rock crusher from the quarry) dominate the raw data (Figure 3). Previous studies in the area showed that the base of the Chalk Group at approximately 900 m produced a strong reflection at 600 ms in the parallel seismic profiles (Lykke-Andersen and Surlyk, 2004; Nielsen et al., 2011). The BC reflection was used to ensure accuracy of the applied processing steps, which are summarized in Table 2. A smooth crooked CDP line with three control points, following the curvature of the road was used for the data processing. Different binning geometries and sizes were tested to find the optimum resolution and fold.

To provide input for refractions statics, first breaks were first picked automatically and later manually inspected and corrected wherever needed to estimate a two-layer refraction static model removing an approximately 6 m weathered quaternary layer with a velocity model ranging from 940 to 1045 m/s. The improvement in the continuity of the BC Group reflection after the refraction static correction is remarkable when comparing Figure 3c and 3d as well as when carefully inspecting the first breaks. Furthermore, an elevation static to a fixed datum of 36 m was applied to account for the high elevations on the northernmost part of the profile. In the

Table 2. Processing steps.

Step	Parameters
	Prestack
1)	Read SEGD-data
2)	Separation of the vertical component of 3C MEMS
3)	Vertical stack ($N = 3$)
4)	Add binning geometry (CDP bin size 1 m, crooked line)
5)	Trace edit (removing dead and noisy) traces
6)	Average amplitude balancing to 1.00
7)	f-k filter to remove ground roll and strong side noise
8)	Band-pass filter (20–40–250–300 Hz)
9)	Spectral balancing with 50–70–250–300 Hz Window = 30 Hz
10)	Refraction statics 940–1045 m/s (approximately 6 m removed)
11)	Elevation statics to fixed datum 36 m (replacement $v = 1400$ m/s)
12)	Deconvolution 13 ms gap
13)	AGC 50 ms
14)	Residual statics
15)	Velocity analysis
16)	NMO correction 100% stretch mute
17)	Stacking
	Post-stack
18)	Band-pass filter 30–45–180–220 Hz
19)	f-x deconvolution: 15 traces L-R and R-L
20)	f-k filter
21)	Deconvolution 10 ms gap
22)	Depth conversion

prestack domain, an f-k filter was applied to partly attenuate strong surface waves. This was then followed by a band-pass filter to reduce low-frequency noise (Figure 3c). A final surface-consistent residual static correction was applied, linked to the NMO velocity to improve the continuity of the reflections. The stretch mute was chosen rather high (100%) to be able to image the very near-surface structures (<20 m depth). The choice of NMO velocities was crucial in obtaining good-quality reflections. The final NMO velocity model ranges from 1300 near the surface to more than 2500 m/s at the BC Group.

In the poststack domain, an additional f-k filter further reduced coherent noise that had remained in the low fold area in the central part of the profile (around CDP 350). A poststack f-x deconvolution filter was used to enhance continuity of the reflections. After this, a poststack deconvolution with a time gap of 10 ms reduced cyclic features and ringing events judged to be in the data. Migration for this short and predominantly horizontally layered section was neglected.

RESULTS

As a basis for stratigraphic and lithologic ties of the upper 450 m of the succession, log and core data from the Stevns-1 borehole are available (Figure 4) (Rasmussen and Surlyk, 2012; Surlyk et al., 2013). The borehole is located less than 19 m east of the seismic line and is well-described in terms of facies and stratigraphy by Rasmussen and Surlyk (2012); hence, due to the very close proximity, the tie to the seismic data is well-substantiated. Furthermore, a detailed analysis of the depositional history of the upper Campanian-Maastrichtian chalk based on the Stevns-2 core has been used to support the interpretation (Boussaha et al., 2016, 2017). The interval deeper than 450 m is not drilled at the Stevns Peninsula, but seismic units defined by Lykke-Andersen and Surlyk (2004) in an offshore seismic survey, immediately to the east, can be used to classify the different chalk units.

Based on previously acquired seismic data onshore and offshore of the profile, the base of the Chalk Group (BC) is well-constrained at approximately 900 m (Lykke-Andersen and Surlyk, 2004; Nielsen et al., 2011). Figure 5 shows the final seismic section, imaging the complete Chalk Group all the way down to 900 m in depth. The seismic data show distinctive variations in strength of reflectivity, frequency of bedding, bed dips, and erosional features. The Stevns-1 gamma ray and porosity logs were transferred into the seismic TWT domain and projected onto the seismic line (Figure 5b). The depth-to-time conversion was based on seismic stacking velocities for the upper 30 m, sonic log data were available, and below from the refraction seismic model of Nielsen et al. (2011) (Figure 5).

The BC reflection is a prominent unconformity, which can be observed in the entire Øresund region as a sharp boundary of Upper Cretaceous to likely Lower Cretaceous or Jurassic sandstone (e.g., Erlstrom et al., 2018). The interval between the BC and Base Campanian (BCa) corresponds to unit 1 of Lykke-Andersen and Surlyk (2004). Based on correlation to the Höllviken boreholes in Sweden, it is interpreted to represent Turonian-Coniacian siliceous chalk and Santonian marly chalk (Lykke-Andersen and Surlyk, 2004). The reflection pattern and strength of reflectivity are variable in this interval. The lower 800 ms of the unit appears mostly horizontally layered with a fault pattern with small to no offsets that can only be observed due to amplitude variations. The upper part is composed of three wedge-shaped sedimentary systems of which the lower is dipping and wedging out southward and the overlying is thinning northward to compensate. Within the wedges, the reflection strength increases upward. The Campanian unit from BCa to the apparent Campanian Unconformity (CaU) shows a similar development with a southward-thinning interval above a lower amplitude unit of undulating reflections and southward-directed downlaps. The interval from CaU to the top of Flagbanke (TFb) is

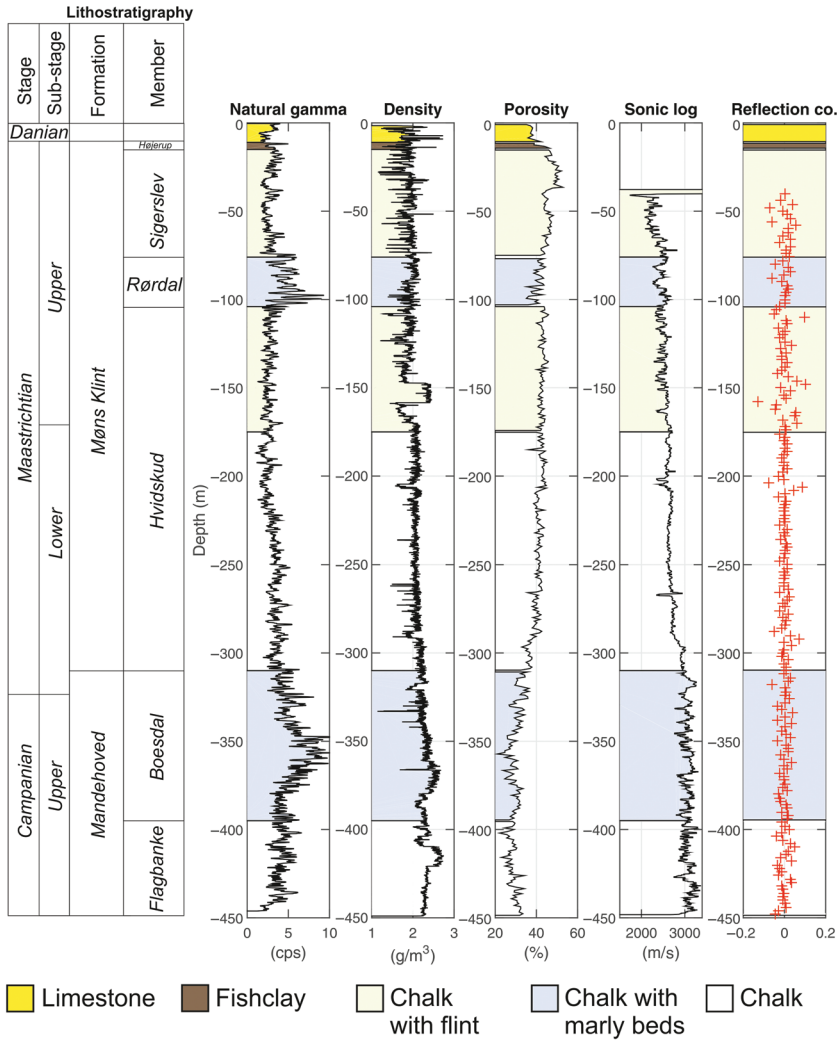

Figure 4. Stevns-1 log data with stratigraphy, lithostratigraphy, and sedimentological classifications from (Rasmussen and Surlyk, 2012). Shown are natural gamma, density, porosity, and P-wave sonic log velocity, along with the calculated reflection coefficient for corresponding depth intervals.

characterized by weak reflectivity with small-scale mounded patterns in the lower part and increasingly parallel reflectivity of higher amplitude upward. The upper part of the Flagbanke unit is represented in the Stevns-1 core and is composed of chalk with some marly beds (Figure 4) (Rasmussen and Surlyk, 2012; Surlyk et al., 2013). From TFb and upward to the Base Hvidskud (BHv), the reflections are predominantly subparallel thinning slightly southward. Undulations are occasionally observed. This succession consists of interbedded chalk, marly chalk, and marl with maximum marl content at approximately 350 m, as indicated by the gamma-ray signal. The Hvidskud Member from BHv to THv (top of Hvidskud) consists of almost-clean chalk with less than 2%–5% noncarbonates in the matrix (Figure 4). In the upper 80 m, flint bands occur regularly. Seismically, the interval is divided into two units. The lower from BHv to Internal Hvidskud (IHv) is characterized by subtle parallel layering and corresponds to the cleanest and most homogeneous chalk intervals in the Stevns-1 and Stevns-2 cores. The occurrence of flint bands at IHv coincides with a clear change of the reflectivity pattern to more chaotic with occasional diffractions and little lateral coherency. The gamma ray indicates a slight increase in clay content (marl) below 175 m as well as decreasing porosity and increasing sonic log velocity (Figure 4). The seismic section of the Rørdal Member between THv and Base of Sigerslev (BS) is not well-expressed and appears as a long-wavelength reflection in the south and as a thinning layered in the north. Small-offset faults are observed in the southern part of the Rørdal Member. The Sigerslev Member ranging from BS to K-Pg (the Cretaceous-Paleogene boundary) at 18–76 m depth shows a different complex reflection pattern with internal undulations and terminations. The BS Member shows onlapping surfaces with southward-directed downlaps of mound-like structures. The K-Pg boundary, expressed by increasing porosity and gamma ray in the wireline log (Figure 4), manifests itself as a strong reflection at 30 ms and can be traced throughout the whole section, although it is interrupted by the low fold around CDP 350 (Figure 5). The boundary undulates slightly along the profile and is interrupted by a fault in the northern part. Throughout the profile, several faults that can be traced only in one or two stratigraphic units are observed. The faults have small to no offsets and are characterized by a low-energy seismic signal and cluster predominantly in the center to northern half of the profile.

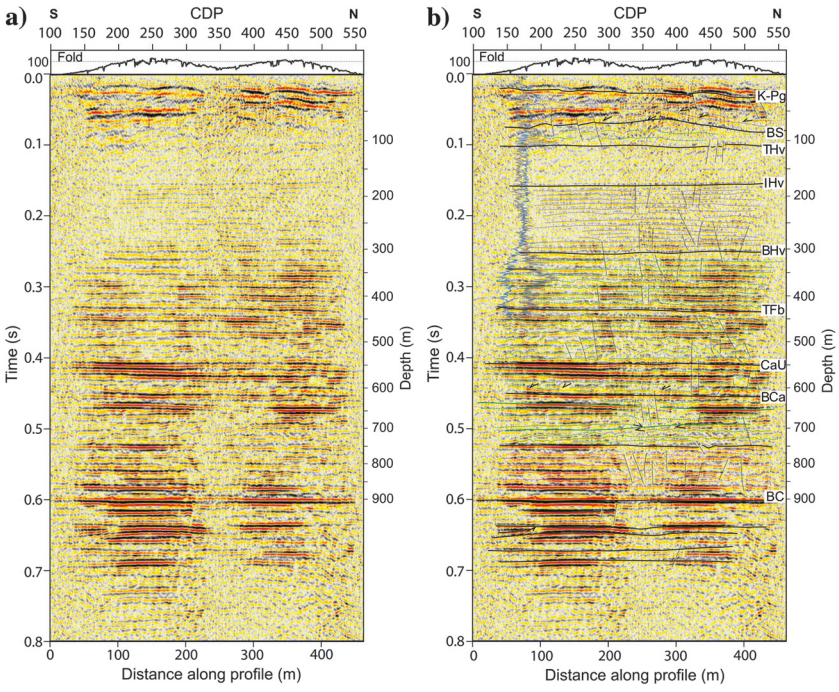

Figure 5. Final stacked section (a) before and (b) after interpretation. The secondary *y*-axis is depth calculated using refraction velocity model (below 30 m), constrained by the borehole data where available, and by Nielsen et al. (2011) below the borehole. Three marker horizons were used to make sure the time-to-depth conversion was done correctly. These were the BC Group at 600 ms (900 m depth), CaU at approximately 400 ms (550 m depth) and the K-Pg boundary at approximately 18 m depth. Abbreviations in (b): K-Pg: Cretaceous Paleogene boundary; BS: Base of the Sigerslev member; THv: Top of Hvidskud; IHv: Internal Hvidskud; BHv: Base of Hvidskud; TFb: Top of Flagbanke; CaU: Campanian Unconformity; BCa: Base of Campanian; and BC: Base of Chalk.

DISCUSSION

Data quality

Despite being acquired with little expense, the presented profile shows excellent data quality and successfully images the heterogeneous Chalk Group with a great level of detail. A neighboring profile shown in Nielsen et al. (2011) (Figure 6) represents the typical data quality achieved in onshore studies of the Chalk Group. The 7 km long reflection seismic line was acquired 800 m west of our profile (Figure 1). This data set was acquired in 2006 using a IVI mini Vib with a 4 s long sweep in the range of 10–500 Hz (Figure 6b). The spread consisted of 96 planted geophones in 5 m intervals resulting in 2.5 m CDP spacing. After processing, the peak frequency was 100 Hz. Figure 6a shows the northern 450 m of the profile at the same scale as our seismic section.

We argue that the main features of the two profiles are consistent, although internal reflectivity is imaged in greater detail in our data. Consistent reflections in both data sets are the BC at 600 ms and the reflectivity patterns between 400 and 500 ms and 250 and 400 ms. This indicates that there are comparably stronger impedance contrasts at these boundaries. However, internal reflectivity within the different units, including terminations, layering, and mounded structures, are significantly better resolved in the new data. The Hvidskud part of the Chalk Group shows internal fine layering with high resolution in our data, which has not been imaged in other data sets. Hence, the presented acquisition setup for this field site excels by resolution and is comparable in the penetration depth. Due to the fundamentally different source and receiver configurations, it is not clear which effect mainly causes differences in data quality, and a direct comparison of source alone or receiver alone is not feasible. However, this data set shows how a small and easy-to-handle impact source with denser receiver spacing, using conventional geophones and MEMS, provides not only comparable data quality, but also even enables imaging of internal structures at higher resolution,

while still being able to image down to the BC Group. This is supported by the study by Almholt et al. (2013), who use a similar acquisition setup with a low energy source and high receiver density, in an area where the Chalk Group is of approximately half the thickness.

Exclusion of the 48 planted 10 Hz vertical geophones connected to wireless units along the whole profile length leads to a reduction of the reflection continuity in the low-fold area (Figure 7). The differences are more prominent when looking in detail at the central part of the profile where the fold decreases dramatically (Figure 7b) compared with the combined data sets (Figure 7c). This illustrates that the wireless geophone units have a significant impact on the data quality in terms of fold and, therefore, on the signal-to-noise ratio. The shallower the reflection surface, the more important is the effect of adding the wireless geophone units. However, the frequency and resolution seem to be comparable after spectral balancing and deconvolution, which on the one hand validates the combination of both receiver systems, and on the other hand rules out receiver-dependent effects on the data quality in the poststack domain. Using the examples shown here, we argue that using the current processing approach combining the MEMS and geophone data is not introducing negative effects (i.e., destructive stacking) and appears appropriate in terms of amplitude and phase.

Geologic implications

Though we expected high attenuation of the seismic signal in the Chalk Group (Payne et al., 2007) and limited reflectivity in the clear chalk interval, we find that the Chalk Group is highly heterogeneous in terms of seismic reflection. The impedance contrasts within the Chalk Group appear to be at the recordable limit, suggesting that most of the signal is being transmitted at the boundaries. To better address this issue, we have calculated reflection coefficients with an increment of 5 m for a plane wave, normal-incident reflection, based on the log data from Stevns-1. The reflection coefficient ranges from zero to numerical values of 0.09 (at the Top of Hvidskud

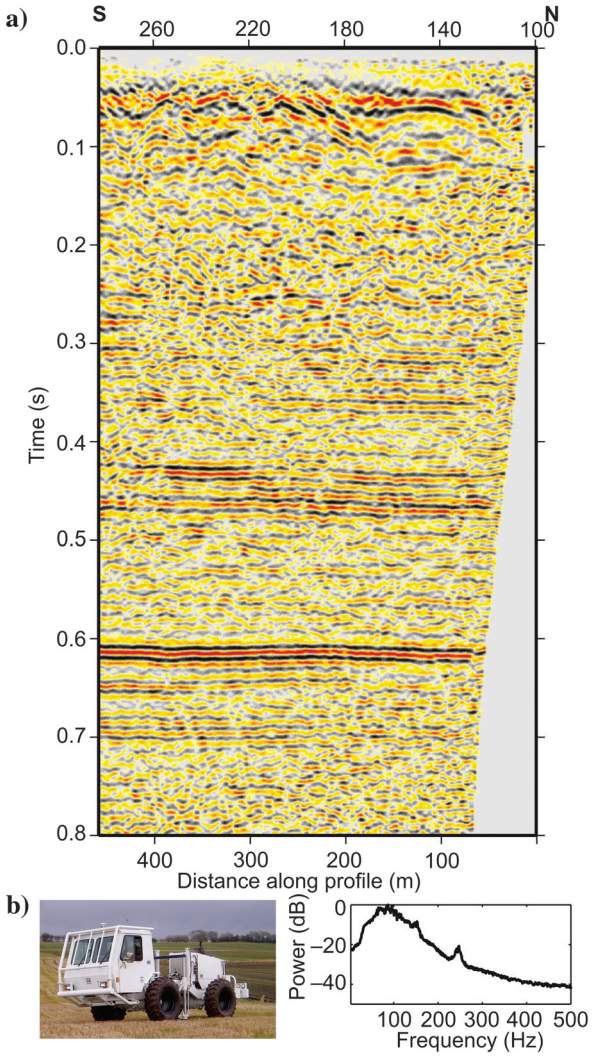

Figure 6. Reflection seismic line published by Nielsen et al. (2011). For comparison, the northern 450 m (equivalent to 180 traces) were cut out, running parallel to the presented profile. The line was acquired with an IVI mini-vib similar to the one shown in (b) with 5 m receiver spacing and 72 channels.

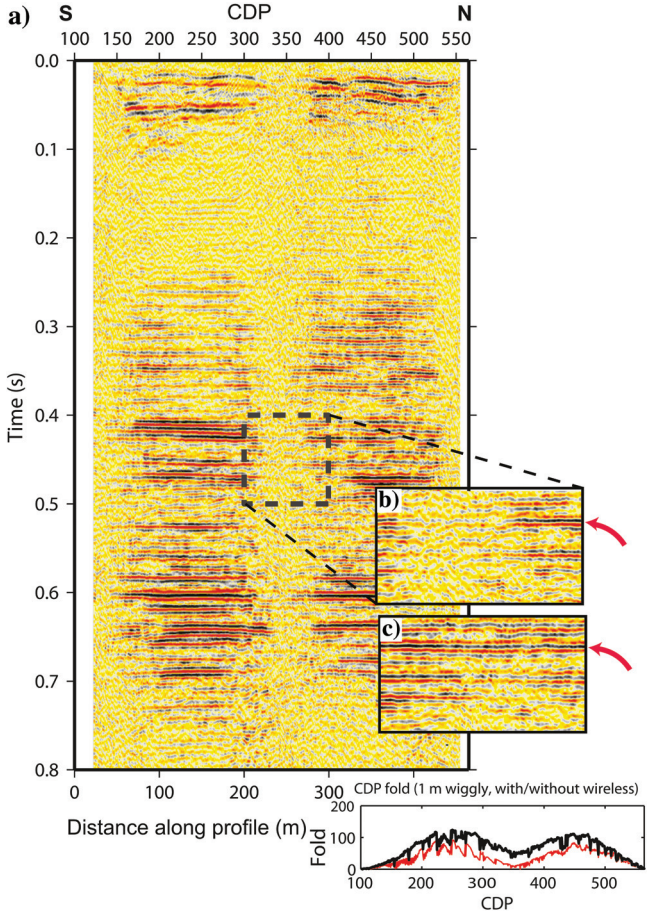

Figure 7. Stacked seismic section only considering the landstreamer and without wireless recorders with planted geophones. A close-up of the low-fold area in the central part of the profile is shown in (b) without and (c) with the wireless recorders. The CDP fold plot is also shown in the bottom of the figure (red without wireless recorders and black with wireless recorders). Note that the obvious improvement has an implication that merging the geophone and MEMS data worked well and did not introduce any negative effect.

member) within the range of the borehole (Figures 4 and 8). Excluded are values around the 150 m density anomaly because this most likely represents a measuring (or calibration) error. However, most of the reflection coefficients lie in an interval from –0.05 to 0.05 (Figure 8). Hence, only a small fraction of the energy is actually being reflected at the individual boundaries inside the Chalk Group. We observe a high dependency of reflection amplitudes from the presence of marl when comparing the gamma ray to the seismic data. Assuming a velocity contrast from 4030 to 3000 m/s at the boundary from chalk to sandstone (Nielsen et al., 2011) and a density contrast of 2.58–2.61 g/m^3, the reflection coefficient at the BC reflection is approximately −0.14. This coincides with a phase shift and the relatively strong reflection observed at the base of the Chalk Group.

In general, we observe that reflectivity increases with marl content, except in the Rørdal Member. Although the Rørdal Member was observed as a cyclic marly chalk/chalk member in other outcrops and boreholes in the Danish Basin (Surlyk et al., 2010), it is not well-expressed in terms of cyclicity in the Stevns-1 borehole. Changes in the clay content are gradual rather than having sharp boundaries. This may be the reason for the Rørdal Member to be less well-expressed in this particular location.

For the first time, a cyclic layering has been imaged within the pure chalk appearing more pronounced below the flint layers of the Hvidskud Member. Silica in the form of isolated flint nodules or a few tens of centimeters thick, more-continuous flint bands do not have a significant enhancing effect on the continuous reflectivity. Rather, the flint-containing part of the Hvidskud Member, where layering is recognizable in the core, is characterized by chaotic reflections and diffractions and little lateral coherency, whereas the white chalk in the lower part of the member appears finely layered in the seismic section (Figures 4 and 5).

The observed CaU may well be connected to intraplate shortening events, changing the basin formation and causing folding and faulting within the area (e.g., Lykke-Andersen and Surlyk, 2004).

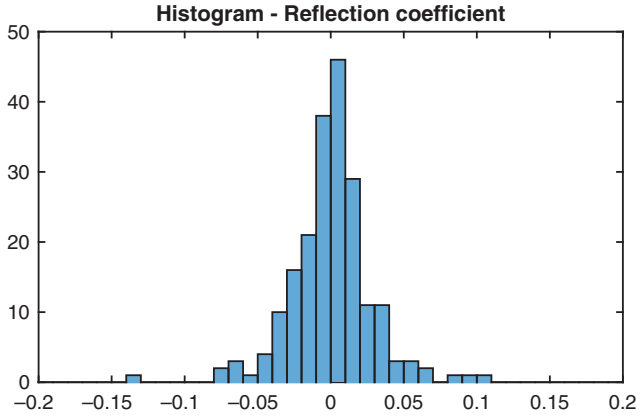

Figure 8. Histogram of the estimated reflection coefficients from the log data assuming a normal incident at every 5 m depth interval (Figure 5). On this basis and the great penetration observed in the data using only a 45 kg accelerated weight-drop, we argue that the reflection coefficients were just big enough to reflect from many boundaries within the Chalk Group, but they were still relatively small; hence, most of the energy is being transmitted to deeper levels. This combined with the high receiver density and broadband data acquisition offered by the MEMS sensors led to successful imaging of the whole Chalk Group to the base at approximately 900 m.

During deposition of the Chalk Group, the Danish Basin underwent several stages of inversion tectonics. Four stages of inversion have been identified in the Danish North Sea and could be related to the study area (e.g., Vejbæk and Andersen, 1987). The most prominent created a basin-wide unconformity during Campanian time and is well-constrained by stratigraphic, 3D seismic, and thermochronologic data (e.g., Vejbæk and Andersen, 2002; Kley and Voigt, 2008; van Buchem et al., 2018).

The observed unconformities with units of opposite-directed trends between the BC and the Base of Campanian might represent changes in the conturite drift system as observed by (Esmerode et al., 2007). Conturite drift systems are observed within the basin in the Santonian to late Campanian successions, forming unconformities, sediment waves, drifts, and moats (Esmerode et al., 2007). Faults observed in the profile show a similar pattern as compared with the polygonal fault structures mapped offshore of Stevns by Moreau et al. (2016).

The study by Nielsen et al. (2004) showed that observed mound structures extending several hundreds of meters in marine seismic data in the Kattegat are unlikely to be of the same origin as the outcropping mound structures at the cliffs of Stevns, concluding that mounds, as observed in the outcrops, could not be resolved by seismic data. This is also in accordance with the vibroseis data from Nielsen et al. (2011) (Figure 6). In our newly acquired data from the site, we were able to map several mound structures of outcrop scale within the Danian as well as in the Sigerlev member. The different widths of the mounds on the northern compared with the southern parts of the profile (i.e., 40–50 m versus 20–25 m accordingly) can be caused by different imaging planes of the mound structures.

In summary, we conclude that the combination of the small impact source (weight-drop) and broadband recording with high CMP fold results in successful imaging of a Chalk Group with relatively low-impedance contrasts. The low-impedance contrasts allow the energy to be transmitted through the Chalk Group, hence the relatively deep depth penetration. All of the results shown indicate that this is likely one of the first times that such a small impact source in a highly noisy environment has enabled such high-resolution imaging thanks to the setup used in the study.

CONCLUSION

We have acquired a high-resolution, 2–4 m receiver and source spacing, 450 m long seismic profile over a section of the Chalk Group, one of the main North Sea reservoir rock types, using a weight-drop seismic source with a receiver setup consisting of a combination of a MEMS-based landstreamer and geophones with wireless recorders. The combination of a landstreamer and planted geophones enabled us to save time compared with the more ideal scenario of moving the streamer to an additional position with more overlap, to increase the fold in the central part of the profile. Based on our results, we conclude

- Despite being acquired at a low cost and short time (a day of acquisition with all logistics), the presented profile shows excellent data quality and great success in imaging the heterogeneous Chalk Group in detail.
- Marl-rich successions appear generally more reflective.
- For the first time, we can image finely layered structures within the white chalk member (Hvidskud).

- The flint bands in this succession do not seem to result in a parallel-layered reflection characteristics. Rather, they cause diffractions and diffuse reflection patterns of limited lateral continuity.
- Unconformities were observed within the Santonian to Campanian unit indicative of intraplate shortening events and changes in conturite drift systems.
- For the first time, Danian and Upper Cretaceous mounds with comparable extent as mounds on the outcrop-scale were imaged by high-resolution seismics.

ACKNOWLEDGMENTS

The seismic survey was conducted during a Ph.D.-week course sponsored by the Faculty of Science, University of Copenhagen. We thank several Ph.D. students from the University of Copenhagen, Denmark, and Uppsala University, Sweden for their contributions to the data acquisition. The landstreamer system was developed by Uppsala University through supports from Formas (project 252-2012-1907), BeFo, SBUF, Skanska, Geological Survey of Sweden, FQM, and NGI for which we are grateful. We want to thank the reviewer I. Morozov and one anonymous reviewer, whose comments helped in improving the manuscript. This study was financed by the Danish Hydrocarbon Research and Technology Center.

DATA AND MATERIALS AVAILABILITY

Data associated with this research are confidential and cannot be released.

REFERENCES

Abramovitz, T., C. Andersen, F. Jakobsen, L. Kristensen, and E. Sheldon, 2010, 3D seismic mapping and porosity variation of intra-chalk units in the southern Danish North Sea: Petroleum Geology Conference Proceedings, Geological Society of London, 537–548.

Almholt, A., R. Wisen, R. B. Jprgensen, J. Ringgaard, and U. T. Nielsen, 2013, High resolution 2D reflection seismic land streamer survey for groundwater mapping: Case study from southeast Denmark: 83rd Annual International Meeting, SEG, Expanded Abstracts, 1894–1898, doi: 10.1190/segam2013-1353.1.

Anderskouv, K., T. Damholt, and F. Surlyk, 2007, Late Maastrichtian chalk mounds, Stevns Klint, Denmark combined physical and biogenic structures: Sedimentary Geology, **200**, 57–72, doi: 10.1016/j.sedgeo.2007.03.005.

Anderson, J., 1999, The capabilities and challenges of the seismic method in chalk exploration: 5th Petroleum Geology of Northwest Europe Conference, Geological Society of London, 939–947.

Baker, G., D. Steeples, C. Schmeissner, and K. Spikes, 2000, Collecting seismic-reflection data from depths shallower than three meters: Symposium on the Application of Geophysics to Engineering and Environmental Problems, SEG, 1207–1214.

Bergman, B., C. Juhlin, and H. Palm, 2002, High-resolution reflection seismic imaging of the upper crust at Laxemar, southeastern Sweden: Tectonophysics, **355**, 201–213, doi: 10.1016/S0040-1951(02)00142-7.

Bjerager, M., and F. Surlyk, 2007, Danian cool-water bryozoan mounds at Stevns Klint, Denmark: A new class of non-cemented skeletal mounds: Journal of Sedimentary Research, **77**, 634–660, doi: 10.2110/jsr.2007.064.

Boussaha, M., N. Thibault, K. Anderskouv, J. Moreau, and L. Stemmerik, 2017, Controls on upper Campanian-Maastrichtian chalk deposition in the eastern Danish Basin: Sedimentology, **64**, 1998–2030, doi: 10.1111/sed.12386.

Boussaha, M., N. Thibault, and L. Stemmerik, 2016, Integrated stratigraphy of the late Campanian-Maastrichtian in the Danish Basin: Revision of the Boreal calcareous nanno-fossil zonation: Newsletters on Stratigraphy, **49**, 337–360, doi: 10.1127/nos/2016/0075.

Brodic, B., A. Malehmir, C. Juhlin, L. Dynesius, M. Bastani, and H. Palm, 2015, Multicomponent broadband digital-based seismic landstreamer for near-surface applications: Journal of Applied Geophysics, **123**, 227–241, doi: 10.1016/j.jappgeo.2015.10.009.

Erlstrom, M., L. Boldreel, S. Lindstrom, L. Kristensen, A. Mathiesen, M. Andersen, E. Kamla, and L. Nielsen, 2018, Stratigraphy and geothermal assessment of Mesozoic sandstone reservoirs in the presund basin — Exemplified by well data and seismic profiles: Bulletin of the Geological Society of Denmark, **66**, 123–149.

Erlstrom, M., S. Thomas, N. Deeks, and U. Sivhed, 1997, Structure and tectonic evolution of the Tornquist zone and adjacent sedimentary basins in Scania and the southern Baltic Sea area: Tectonophysics, **271**, 191–215, doi: 10.1016/S0040-1951(96)00247-8.

Esmerode, E. V., H. Lykke-Andersen, and F. Surlyk, 2007, Ridge and valley systems in the upper Cretaceous chalk of the Danish Basin: Contourites in an Epeiric sea: Geological Society of London, Special Publications, 265–282.

Fabricius, I. L., 2003, How burial diagenesis of chalk sediments controls sonic velocity and porosity: AAPG Bulletin, **87**, 1755–1778, doi: 10.1306/06230301113.

Frykman, P., 2001, Spatial variability in petrophysical properties in upper Maastrichtian chalk outcrops at Stevns Klint, Denmark: Marine and Petroleum Geology, **18**, 1041–1062, doi: 10.1016/S0264-8172(01)00043-5.

Hjuler, M., and I. L. Fabricius, 2009, Engineering properties of chalk related to diagenetic variations of upper Cretaceous onshore and offshore chalk in the North Sea area: Journal of Petroleum Science and Engineering, **68**, 151–170, doi: 10.1016/j.petrol.2009.06.005.

Inazaki, T., 2004, High-resolution seismic reflection surveying at paved areas using an S-wave type land streamer: Exploration Geophysics, **35**, 1–6, doi: 10.1071/EG04001.

Kaiser, A., H. Horstmeyer, A. G. Green, F. Campbell, R. Langridge, and A. McClymont, 2011, Detailed images of the shallow Alpine fault zone, New Zealand, determined from narrow-azimuth 3D seismic reflection data: Geophysics, **76**, no. 1, B19–B32, doi: 10.1190/1.3515920.

Kley, J., and T. Voigt, 2008, Late Cretaceous intraplate thrusting in central Europe: Effect of Africa-Iberia-Europe convergence, not Alpine collision: Geology, **36**, 839–842, doi: 10.1130/G24930A.1.

Lykke-Andersen, H., and F. Surlyk, 2004, The Cretaceous-Palaeogene boundary at Stevns Klint, Denmark: Inversion tectonics or sea-floor topography?: Journal of the Geological Society, **161**, 343–352, doi: 10.1144/0016-764903-021.

Malehmir, A., G. Maries, E. Backstrom, M. Schon, and P. Marsden, 2017, Developing cost-effective seismic mineral exploration methods using a landstreamer and a drophammer: Scientific Reports, **7**(1), 10325. doi: 10.1038/s41598-017-10451-6.

Malehmir, A., S. Wang, J. Lamminen, B. Brodic, M. Bastani, K. Vaittinen, C. Juhlin, and J. Place, 2015, Delineating structures controlling sandstone-hosted base-metal deposits using high-resolution multicomponent seismic and radio-magnetotelluric methods: A case study from Northern Sweden: Geophysical Prospecting, **63**, 774–797, doi: 10.1111/1365-2478.12238.

Maxwell, P., J. Tessman, and B. Reichert, 2001, Design through to production of a MEMS digital accelerometer for seismic acquisition: Land seismic surveys and technology: First Break, **19**, 141–144.

Miller, R., S. Pullan, J. Waldner, and F. Haeni, 1986, Field comparison of shallow seismic sources: Geophysics, **51**, 2067–2092, doi: 10.1190/1.1442061.

Montazeri, M., A. Uldall, J. Moreau, and L. Nielsen, 2018, Pitfalls in velocity analysis for strongly contrasting, layered media — Example from the Chalk Group, North Sea: Journal of Applied Geophysics, **149**, 52–62, doi: 10.1016/j.jappgeo.2017.12.003.

Moreau, J., M. Boussaha, L. Nielsen, N. Thibault, C. V. Ullmann, and L. Stemmerik, 2016, Early diagenetic evolution of chalk in eastern Denmark: The Depositional Record, **2**, 154–172, doi: 10.1002/dep2.19.

Nielsen, L., L. O. Boldreel, T. M. Hansen, H. Lykke-Andersen, L. Stemmerik, F. Surlyk, and H. Thybo, 2011, Integrated seismic analysis of the Chalk Group in eastern Denmark: Implications for estimates of maximum palaeo-burial in southwest Scandinavia: Tectonophysics, **511**, 14–26, doi: 10.1016/j.tecto.2011.08.010.

Nielsen, L., L. O. Boldreel, and F. Surlyk, 2004, Ground-penetrating radar imaging of carbonate mound structures and implications for interpretation of marine seismic data: AAPG Bulletin, **88**, 1069–1082, doi: 10.1306/02230403070.

Payne, S., M. Worthington, N. Odling, and L. West, 2007, Estimating permeability from field measurements of seismic attenuation in fractured chalk: Geophysical Prospecting, **55**, 643–653, doi: 10.1111/j.1365-2478.2007.00643.x.

Rasmussen, S. L., and F. Surlyk, 2012, Facies and ichnology of an upper Cretaceous chalk contourite drift complex, eastern Denmark, and the validity of contourite facies models: Journal of the Geological Society, **169**, 435–447, doi: 10.1144/0016-76492011-136.

Smit, F., F. van Büchern, J. Holst, M. Lüthje, K. Anderskouv, N. Thibault, G. Buijs, M. Welch, and L. Stemmerik, 2018, Seismic geomorphology and

origin of diagenetic geobodies in the upper Cretaceous Chalk of the North Sea Basin (Danish Central Graben): Basin Research, **30**, 895–925, doi: 10.1111/bre.12285.

Surlyk, F., 1997, A cool-water carbonate ramp with bryozoan mounds: Late Cretaceous-Danian of the Danish Basin, 56th ed.: Special Publications of SEPM 1, 293–307.

Surlyk, F., S. L. Rasmussen, M. Boussaha, P. Schi0ler, N. H. Schovsbo, E. Sheldon, L. Stemmerik, and N. Thibault, 2013, Upper Campanian-Maastrichtian holostratigraphy of the eastern Danish Basin: Cretaceous Research, **46**, 232–256, doi: 10.1016/j.cretres.2013.08.006.

Surlyk, F., L. Stemmerik, M. Ahlborn, R. Harlou, B. W. Lauridsen, S. L. Rasmussen, N. Schovsbo, E. Sheldon, and N. Thibault, 2010, The cyclic Rørdal Member: A new lithostratigraphic unit of chronostratigraphic and palaeoclimatic importance in the upper Maastrichtian of Denmark: Bulletin of the Geological Society of Denmark, **58**, 89–98.

Thomsen, E., 1976, Depositional environment and development of Danian bryozoan biomi-crite mounds (Karlby Klint, Denmark): Sedimentology, **23**, 485–509, doi: 10.1111/j.1365-3091.1976.tb00064.x.

Thybo, H., 2001, Crustal structure along the EGT profile across the Tornquist fan interpreted from seismic, gravity and magnetic data: Tectonophysics, **334**, 155–190, doi: 10.1016/S0040-1951(01)00055-5.

van Buchem, F. S. P., F. W. H. Smit, G. J. A. Buijs, B. Trudgill, and P.-H. Larsen, 2018, Tectonostratigraphic framework and depositional history of the Cretaceous-Danian succession of the Danish Central Graben (North Sea): New light on a mature area: Geological Society of London, Petroleum Geology Conference Series, 946.

van der Veen, M., and A. G. Green, 1998, Land streamer for shallow seismic data acquisition: Evaluation of Gimbal mounted geophones: Geophysics, **63**, 1408–1413, doi: 10.1190/1.1444442.

Vangkilde-Pedersen, T., J. F. Dahl, and J. Ringgaard, 2006, Five years of experience with landstreamer vibroseis and comparison with conventional seismic data acquisition: 19th Symposium on the Application of Geophysics to Engineering and Environmental Problems, 1086–1093.

Vejbæk, O., and C. Andersen, 2002, Post mid-Cretaceous inversion tectonics in the Danish Central Graben — Regionally synchronous tectonic events: Bulletin of the Geological Society of Denmark, **49**, 93–204.

Vejbæk, O. V., and C. Andersen, 1987, Cretaceous-early Tertiary inversion tectonism in the Danish Central trough: Tectonophysics, **137**, 221–238, doi: 10.1016/0040-1951(87)90321-0.

Vejbæk, O. V., T. Bidstrup, P. Britze, M. Erlstrôm, E. S. Rasmussen, and U. Sivhed, 2007, Chalk depth structure maps, central to eastern North Sea, Denmark: Geological Survey of Denmark and Greenland Bulletin, **13**, 9–12.